



PRACTICAL PRESCRIPTION OF VARIABLE RATE FERTILIZATION MAPS USING REMOTE SENSING BASED YIELD POTENTIAL

Maria Calera¹, Carmen Plaza¹, Jaime Campoy³, Julio Villodre³, Sergio Sánchez³, Nuria Jimenez², Isidro Campos^{1,3}, Vicente Bodas², Alfonso Calera³, Anna Osann^{1,3}, Horacio López⁴.

¹AGRISAT-IBERIA, Pol. Campollano, Av, 3^a N 27, Albacete, (Spain)

²ALIARA AGRÍCOLA, C/Matadero 11, Talavera de la Reina, (Spain)

³GIS and Remote Sensing Group. Universidad de Castilla-La Mancha. Campus Universitario. Albacete (Spain).

⁴ Regional Agronomic Institute (ITAP), Pol. Campollano, Segunda Avenida, 61, Albacete (Spain)

**A paper from the Proceedings of the
14th International Conference on Precision Agriculture
June 24 – June 27, 2018
Montreal, Quebec, Canada**

Abstract. *This paper describes a practical approach for the prescription of variable rate fertilization maps using remote sensing data (RS) based on satellite platforms, Landsat 8 and Sentinel-2 constellation. The methodology has been developed and evaluated in Albacete, Spain, in the framework of the project FATIMA (<http://fatima-h2020.eu/>). The global approach considers the prescription of N management prior to the growing season, based on a spatially distributed N balance. Although the diagnosis of N status showed promising results, the necessity of prognostic tools for N management is undiscussed for crops like wheat. The spatially distributed N balance relies in the use of management zone maps (MZM) based on temporal series of RS data. The MZMs are calculated for previous growing seasons, based on the up-to-date RS approaches to estimate yield and biomass, and captures the within-field variability of crop production. Thus, the classical N balance model is used to calculate the N requirements at pixel scale, varying the soil properties when the input data are available and the target yield according to the MZM. It has been implemented trials and demonstration activities in commercial fields in the study area, analyzing the performance of the proposed fertilization strategies. The preliminary results indicated the possible optimization of the N application, maintaining or increasing the crop productivity and reaching the higher levels of yield quality in the area.*

Keywords. Fertimaps©, NDVI, Landsat 8, Sentinel 2, Nitrogen, VRT fertilization.

The authors are solely responsible for the content of this paper, which is not a refereed publication.. Citation of this work should state that it is from the Proceedings of the 14th International Conference on Precision Agriculture. EXAMPLE: Lastname, A. B. & Coauthor, C. D. (2018). Title of paper. In Proceedings of the 14th International Conference on Precision Agriculture (unpaginated, online). Monticello, IL: International Society of Precision Agriculture.

1. Introduction

The agricultural activity is facing severe challenges and requires the implementation of optimizing strategies. While the increasing use of inputs such as fertilizers have played a major role in increasing the supply of food (Goulding et al., 2008), the current demand for resources in agriculture is unsustainable (FAO, 2015, 2014). On these conditions, the adoption of sustainable intensification guidelines in agriculture (SI) is one of the most consensual strategies, recognized by different international organizations including FAO (Buckwell et al., 2014; FAO, 2014). SI is defined by Garnett et al. (2013) as “to produce more outputs with a more efficient use of all inputs (including knowledge and know-how) on a durable basis”. Under these conditions, our objective must be to achieve optimized yield in quantity, quality or farm income, with a minimum use of inputs and conserving the environment. The analysis and methodologies presented on this work pursue the optimization of the use of external nitrogen input in intensive production systems paying special attention to the management of land heterogeneity.

The management of the land variability, adapting the inputs to the actual crop requirements across time and space is the paradigm of precision agriculture (PA). The adoption of these technologies rests on the development of feasible methods for the characterization of the heterogeneity, the adaptation of the external inputs to the known variability and the recommendation of corrective actions, if possible. In this sense, previous researches are oriented to the identification of N deficiencies during the growing season (diagnostic approaches) and successful experience can be found in the literature (Cilia et al., 2014; Clevers and Gitelson, 2013; Gitelson et al., 2005; Hatfield et al., 2008). These indicators are effective after the initial crop stages, when the crop is well established covering most of the ground but for wheat and many herbaceous crops, the common fertilization strategies allow for few opportunities to manage the within-field variability after the tillering stage. Thus, it is necessary to develop specific methods for the assessment of N fertilization in early stages (Cilia et al., 2014) and previous research proposed the prescription of the fertilization delineating management zone maps (MZM) based on geolocated data (Derby et al., 2007; Peralta et al., 2015)

This document aims to present operational approaches for the quantification of the spatial variability of crop growth, the spatialized recommendation of nitrogen fertilization. The proposed methodology is innovative in the use of space RS temporal series as a proxy of the crop response to soil fertility factors. The most recent missions such as Sentinel 2 offers a great potential on these tasks providing i) high temporal resolution which makes it possible to follow the vegetation during the critical stage revealing the coupled effect of the soil, water and nitrogen on the crop development, ii) high spatial resolution (10m) sufficient for the spatial variation of the fertilization rates. This document, presents the rationale of those methods and the trials and demonstration activities in commercial fields. The experiences presented here were obtained for wheat, although similar experiences in other crops are currently on development.

2. Methodology

The methods described in this work follows two main principles for the optimization of nitrogen use based on the prescription of variables rates based on management zone maps (MZM) describing the spatial variability of the expected crop yield. This approach is based on the classical principles of nitrogen balance and make use of RS data for the estimation of the required variables at high temporal resolution and the required spatial scale.

2.1. Nitrogen prescription based on management zone maps and yield potential.

The usual fertilization practice requires the prescription of the N in terms of timing and amount considering the expected yield. The estimation of the crop requirements could vary from the simplest reposition strategies based on the expected nitrogen abstractions to more sophisticated methods based on the balance of N in the soil. The N recommendation is back-calculated from the expected yield and assuming common grain protein contents and a grain N total or N uptake ratio. Additional considerations are the N use efficiency and the N credit from other sources (e.g., previous legume crops, manure, N mineralization, and N in irrigation water). This classical “yield potential approach” does not take into account the within-field yield variability induced by the soil spatial differences in fertility levels and water availability in the soil (Holland and Schepers, 2010).

The proposed approach, RS-based yield potential, follows the classical procedures, taking advantage of accumulated scientific knowledge, but considering each pixel as the minimum unit of information representing the within-field heterogeneity. Thus, the key is to establish the spatial distribution of the expected yield, and the methodology proposed is based on time series of multispectral imagery as presented in the next subsection. The application of the N mass balance at pixel scale requires the soil sampling in the areas delimited in the map of expected yield, so the ground data apprehend the soil heterogeneity in the soil properties. The Figure 1 shows the flow diagram for this procedure. From a practical point of view, it should be noted that the current practices in commercial fields in the study area difficulty consider the systematic measurement of the required variables (mainly mineral N and organic matter) in more than one location. Thus, in this initial experience it has been proposed a simplified approach in which the soil contribution in terms of N was considered homogeneous (Derby et al., 2007) and the main driver of the spatial variability in N requirements is the difference in expected crop yield.

2.1.1. Mapping within-field variability of yield and biomass production.

The basis of several crop growth models to explain the crop evolution and biomass accumulation are the well-known water and light use efficiency principles. These basic processes occur in the soil-plant-atmosphere system and explain the biomass accumulation as the result of transpiration and solar radiation absorbed by plants. The basic assumption is that the rate of biomass accumulation is driven by actual transpiration accounting for the water stress (T_{act}) or light absorbed (APAR), as expressed in the Equation 1 and Equation 2.

$$B = \int WP \cdot T_{act} \cdot dt \quad \text{Equation 1}$$

$$B = \int \epsilon \cdot APAR \cdot K_s \cdot dt \quad \text{Equation 2}$$

where:

B: biomass accumulated in a time t per unit of surface [kg/m²]

WUE/WP: water use efficiency or water productivity [kg of biomass per m³ of water transpired]; crop dependent

ϵ : conversion efficiency of solar radiation into biomass or ratio of chemical energy equivalent of absorbed PAR [kg/MJ]; crop dependent

APAR, absorbed PAR [MJ/m²]

K_s : water stress coefficient [dimensionless]. It requires a soil water balance in the root soil layer.

T_{act} , actual transpiration [m^3 water transpired/ m^2]

One of the main weakness for the assessment of the in-field variability in yield and biomass is the determination of the crop transpiration and light interception, or specifically the transpiration coefficient (K_t) and the fraction of photosynthetic active radiation absorbed by the vegetation ($fPAR$) used in the estimation of these variables, see Equations 3 and 4.

$$T_{act} = ETo \cdot K_s \cdot K_t \quad \text{Equation 3}$$

$$APAR = PAR_{in} \cdot fPAR \quad \text{Equation 4}$$

where:

ETo : reference crop evapotranspiration [mm/day]

K_t : transpiration coefficient [dimensionless]

PAR_{in} , incident PAR [MJ/m^2]

$fPAR$: fraction of photosynthetic active radiation absorbed by the vegetation [dimensionless].

On the described conceptual basis, it has been implemented a direct remote sensing-based approach for monitoring biomass growth, with the aim to be operational in the description of the within-field variability. This approach integrates time series of multispectral imagery into the crop growth models, allowing the estimation of biomass at pixel scale. The approach implemented is based on the relationship between K_t or $fPAR$ and the normalized difference vegetation index (NDVI). In this work, we used the K_t -NDVI relationship proposed by Duchemin et al. (2006) and the $fPAR$ -NDVI relationship proposed by Asrar et al. (1984) for wheat, see Equations 5 and 6. Details about this procedure and the evaluation of the performance of the model for wheat in the study area can be found in Campos et al. (2018). The simulated values of ground biomass and yield calculated following the methodology described requires the knowledge of the spatial distribution of the water stress. The estimation of K_s is not possible in operational applications, because it requires the simulation of the water balance at pixel scale, and the soil information is not generally available. Thus we propose a simplification in which the actual distribution of the water stress is considered unknown. The exactitude of these estimates was analyzed with respect to field measurements of crop aboveground biomass and grain production based on the yield maps obtained by combine-mounted grain yield monitors.

$$K_t = 1.5 \cdot NDVI - 0.2 \quad \text{Equation 5}$$

$$fPAR = 1.25 \cdot NDVI - 0.11 \quad \text{Equation 6}$$

Grain yield production is strongly related with the biomass production although not in an unequivocally way. The crop yield can be estimated as a variable proportion of total aboveground biomass that goes into the harvestable parts depending on the biotic and abiotic stresses, the duration, the severity and the crop physiological stage during the stress period. This proportion is known as harvest index (HI). The reduction in grain yield from stresses occurs because of the reduction of assimilate production during grain filling (Ritchie et al., 1998). We implemented an EO-based approach for the HI estimation following the existing knowledge according to the approach proposed by Sadras and Connor (1991) and reanalyzed by Kemanian et al. (2007). This method is based on the ratio between biomass accumulation after anthesis over the biomass accumulation during the entire growing cycle, this ratio is named θ_B , see Equation 3. The values of HI estimated by the function are limited by the maximum HI attainable for the specie (HI_x) and the minimum HI obtained in source limited conditions (HI_0). Therefore, the developed EO-based approach of HI relies on the estimation of θ_B at pixel scale, by using the procedure for biomass growth during the whole growth cycle above described. In addition to the water stress described before, it is generally accepted that N stresses impact on the biomass accumulation, by lowering

the potential biomass growth rate. Yield decreasing reflects both the decrease on biomass and the decrease on HI. Active ongoing research is being dedicated to understanding how the EO-based models described above can capture the impact of this stress and its influence in terms of within-field variability. An operational alternative is the consideration of a constant HI value at the scale of the field monitored. This assumption could reduce our capability to reflect the actual variability of the crop production, but these initial experiences analyzing the similitudes between maps of potential productivity and the map obtained from ground yield monitors offered promising results (Campos et al., 2017).

$$HI = HI_x - (HI_x - HI_0) \cdot \exp(-k \cdot \theta_B) \quad \text{Equation 3}$$

2.1.2. Remote Sensing-based Management Zone Map

It could be defined the yield potential as the attainable yield for a crop on each point of the field under standard weather and management, mainly irrigation and nutrient practices. The within-field variability of yield potential can be quantified as the ratio between yield in any given location (pixel) over the average yield at field scale. The variability it has been expressed in relative units or in % so the 100% correspond to the average value. The approach developed to obtain the final management zone map (MZM) requires the use of multiannual EO time series. For each campaign, the EO-based methodology provides the spatial distribution of the yield. The analysis of multiannual maps allows to discard the effect of abnormal development, irrigation or fertilization fails, bad crop installation, pests or diseases. An example of the combination of the multiannual maps of potential productivity for the delineation of the management zones is presented in the results section. Once the MZM is selected and the variability is defined for each pixel in the map, the average yield expected at field scale can be distributed according to the estimated variability, compounding the target yield map indicated in the Figure 1.

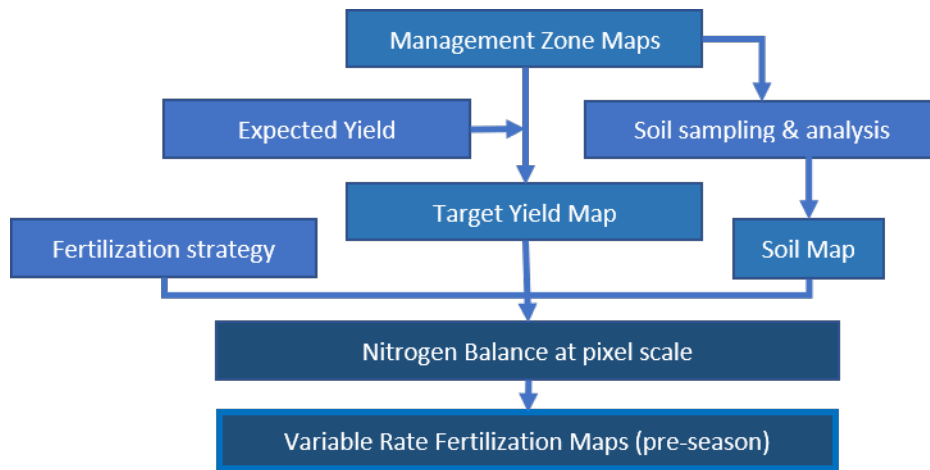


Figure 1. Flow diagram of the elaboration of the VR fertilization maps in pre-season.

3. Results.

3.1. The Remote Sensing-based yield potential map

The results of the model for yield and biomass production are being routinely compared to the variability determined using ground measurements in rainfed and irrigated fields planted with corn and wheat. The data presented in this analysis were obtained in an irrigated commercial field planted with wheat and located in the province of Albacete (Southeast Spain). The climatology in the area is Mediterranean, the mean annual precipitation for the last thirty years is 340 mm and the mean annual temperature is 13.6°C for the same period. In addition to the natural variability of soil fertility, we induced variability in the crop growth varying the N doses proposed by the farmer during the initial stages (crop emergence) in a strip crossing the field. The N dose was reduced in 46 KgN/ha in one strips crossing the fields monitored. The width of the strips (100 m) was sufficient to be monitored with the available images (Landsat and Sentinel 2).

The visual comparison of the maps of measured and modelled yield (Figure 2) indicates the general agreement between both approaches describing the crop heterogeneity at the analyzed scales. The reduction of the nitrogen dose resulted in lower canopy development (lower crop transpiration) and low yield. The comparison of potential biomass production maps and yield maps is limited by our knowledge of the spatial distribution of the HI and the stresses affecting the crop development. The numerical comparison of measured and modelled yield based on constant values of HI resulted in a general good agreement (Campos et al. 2017). However, the detailed analysis of the results pointed to the necessity to adapt the HI values for a better representation of the within-field variability. The model, based on constant values of HI and without considering the spatial distribution of the stresses affecting the biomass production, overestimated the actual yield in the less productive areas. Conversely, the yield modelled in the more productive areas was lower than the yield registered by the monitor. These improvements will be considered in further research. However, the general good agreement obtained in the comparison at the scale of commercial field, and the similitudes of the spatial patterns described by both approaches, let us to suggest the use of the proposed approach for the segmentation of the fields monitored in zones with different yield production and analyzed in the next subsections.

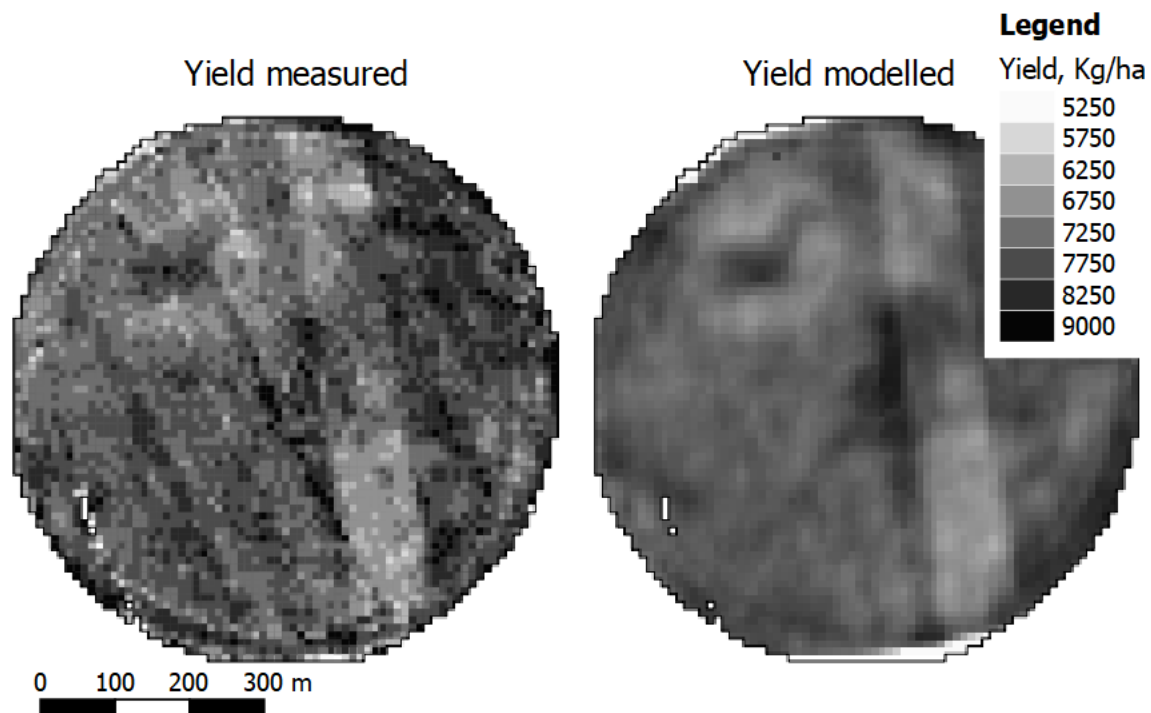


Figure 2. Comparison of measured and modelled yield at the scale of commercial farm. Pixel size 10 m. Adapted from Campos et al. (2017).

3.2. RS-based Management Zone Maps for VR prescription

The annual maps of relative yield potential (RPPM) were analyzed for a commercial field in the Spanish region of Albacete. The field is managed under minimum tillage and irrigated with a central pivot. The total size is 30 ha and the crop rotation in the period monitored was corn-poppy-corn-wheat. The selected RPPM was used to create the variable rate prescription map for the campaign 2017. The Figure 2 represents the RPPM analyzed for the period 2014-2017.

The RPPM obtained during the seasons 2014, 2016 and 2017 presented similar and persistent patterns. The most productive area is in the center of the field, and the potential productivity was about a 9% higher than the field average (see Fig. 3). The less productive area was located in the Northeast of the field (see Fig. 3) and the three maps have an area of transition from the low to the high areas classified as medium potential productivity.

It is important to note that the RPPM obtained in 2015 (poppy) shows the inversion of the patterns. The areas located in the north of the field presented higher potential productivity than in the center of the pivot. The explanation comes from the particularities of the poppy crop. The success of the emergence plays a relevant role for the final productivity and this crop is very sensitive to the limitations to the emergence. The north area presented sandy soils, more favorable for the emergence of the poppy seeds in comparison with the clay soils in the center of the pivot. This map was not considered in the analysis to obtain the final MZM.

Based on these analysis, the map obtained in 2016 (corn) was selected to delimit the management zones and the prescription of the nitrogen doses as presented in the next subsection.

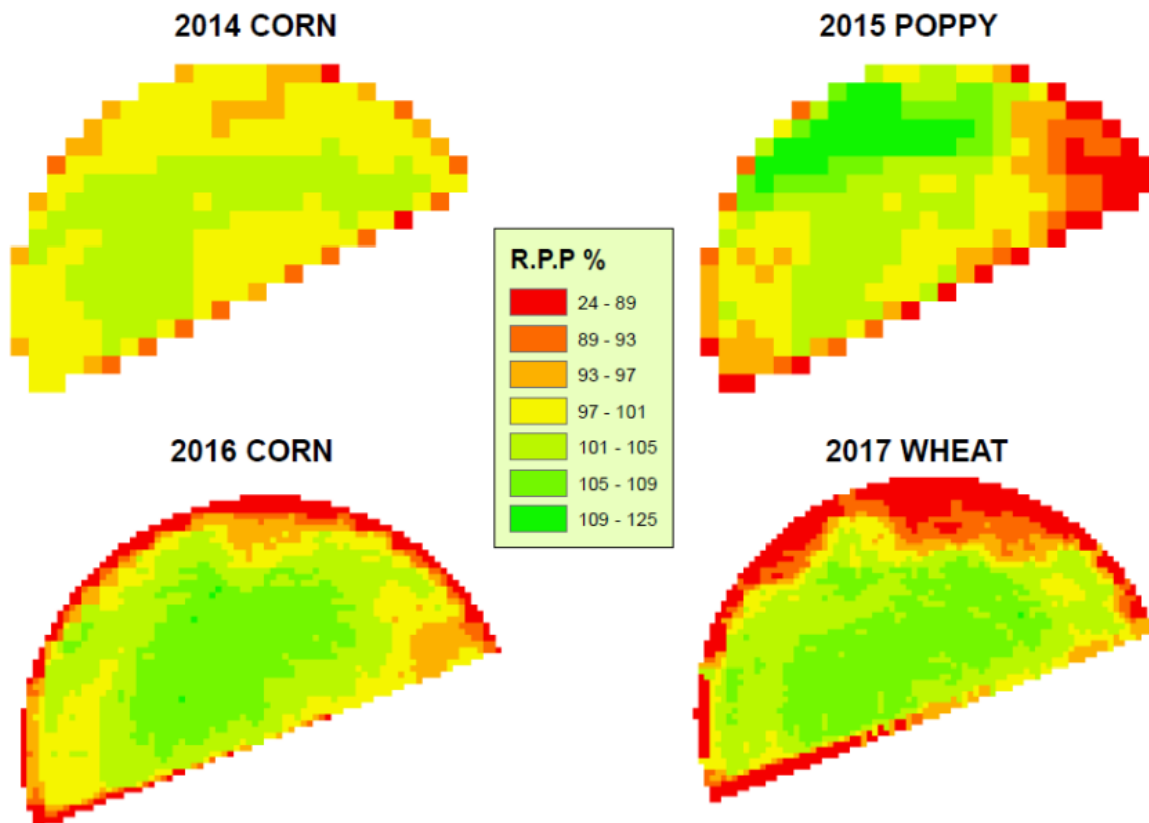


Figure 3. Temporal evolution of the normalized difference vegetation index (NDVI) and the nitrogen nutrition index (NNI) for two areas with different expected productivity. The different areas can be distinguished in the RGB color composition of the Sentinel 2A image obtained in March 30 2017.

3.3. Prescription of VR nitrogen fertilization based on the proposed methodology

This study case exemplified the operational application of the proposed methods in a commercial field planted with bread wheat in the province of Albacete during 2017. The fertilization doses proposed by the farmer, following the local practices, was distributed according to the expected potential productivity. The variable rate fertilization was applied with a common spreader adapted to apply variable rates. The adaptation consisted in GPS monitor where the prescription maps can be uploaded in the proper format and an electronic system connecting the monitor with a piston installed in the fertilizer gate. On this way, the doses can be varied automatically depending on the actual location of the tractor. Due to the limitation of the precision of the existing equipment the spatial distribution of the relative productivity was simplified in a MZM with three different areas and consequently three different doses of N was applied in each application.

The MZM, Figure 4, indicates three areas with well contrasted differences. The Northern area of the field was classified as low productive area, being the relative potential productivity lower than the 98.55% of the field average. The center of the pivot was classified as high productive area being the potential productivity higher than 102.5%. The rest of the field was considered as medium potential productivity. The variability of the crop productivity was the result of the difference in the length of the crop growing cycle. These differences were detected during the previous growing seasons and can be observed in the NDVI curves obtained during the growing season analyzed (2017), see Figure 5.

The N prescribed in each area was estimated according with the fertilization proposed by the farmer, the expected productivity and the characteristics of the spreader. The dose of N prescribed in the area with medium productivity was 264KgN/ha, 244kgN/ha in the area with low productivity and 284KgN/ha in the areas with high expected productivity. The fertilization was divided in four applications following the local practices and the variable rate fertilization was applied in the first and second top-dressing. The doses in both applications were 70 KgN/ha in the area with medium production, 60 KgN/ha in the areas with low productivity and 80 KgN/ha in the areas with high productivity. The average dose corresponds to 24 KgN/T of grain according to the expected production, and it is within the ranges used in the area for high quality wheat. The final production was 10.5 T/ha and the average protein content was 14.1 %.

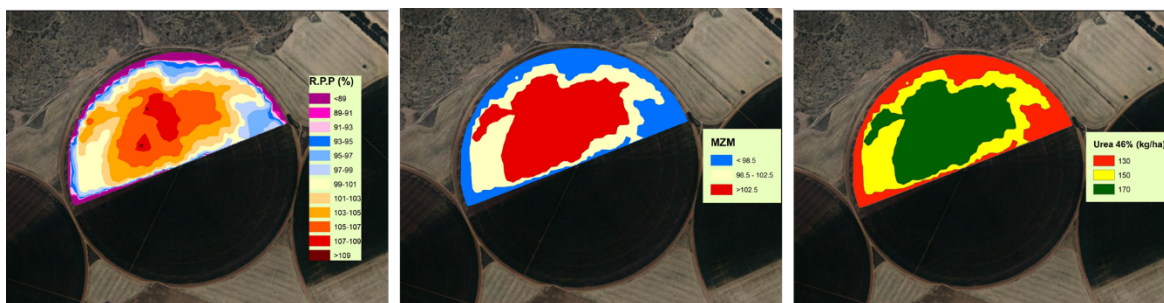


Figure 4. Management Zone Map of the field 2 and nitrogen doses proposed for each area.

Conclusion or Summary

This work analyzed the use of current remote sensing platforms for the operation application of variable rate fertilization. The proposed approach is centered in the prescription of the nitrogen necessities prior to the growing season and further analysis will consider the continuous monitoring of nitrogen status based exclusively in remote sensing data. The study cases analyzed in this work highlight the capability of the potential productivity maps to delineate areas with well contracted differences in crop growth and persistent patters along several growing seasons. These maps are the basic tool for the delineation of potential productivity maps and the adoption of variable rate fertilization strategies.

Acknowledgements

This research was developed in the framework of the projects HERMANA (HERramientas para el MAnejo sostenible de fertilización Nitrogenada y Agua), funded by the Spanish Ministry Science and Innovation (AGL2015-68700-R) and FATIMA (FARming Tools for external nutrient Inputs and water MAnagement), funded by the European Union's Horizon 2020 research and innovation programme (Grant Agreement N° 633945).

References

- Buckwell, A., Uhre, A.N., Williams, A., Poláková, J., Blum, W.E., Schiefer, J., Lair, G.J., 3, Heissenhuber, A., 4, Schieβl, P., 4, Krámer, C., 4, Haber, and W., 2014. The sustainable intensification of European Agriculture.
- Campos, I., González-Gómez, L., Villodre, J., González-Piqueras, J., Suyker, A., Calera, A., 2018. Remote sensing based crop biomass with water or light-driven crop growth models in wheat commercial fields. *F. Crop Res.*
- Campos, I., González, L., Villodre, J., Calera, M., Campoy, J., Jiménez, N., Plaza, C., Calera, A., 2017. Mapping within-field biomass variability: a remote sensing-based approach. *Adv. Anim. Biosci.* 8, 764–769. <https://doi.org/10.1017/S2040470017000139>
- Cilia, C., Panigada, C., Rossini, M., Meroni, M., Busetto, L., Amaducci, S., Boschetti, M., Picchi, V., Colombo, R., 2014. Nitrogen status assessment for variable rate fertilization in maize through hyperspectral imagery. *Remote Sens.* 6, 6549–6565. <https://doi.org/10.3390/rs6076549>
- Clevers, J.G.P.W., Gitelson, A.A., 2013. Remote estimation of crop and grass chlorophyll and nitrogen content using red-edge bands on Sentinel-2 and -3. *Int. J. Appl. Earth Obs. Geoinf.* 344–351, 23.
- Derby, N.E., Casey, F.X.M., Franzen, D.W., 2007. Comparison of nitrogen management zone delineation methods for corn grain yield, in: *Agronomy Journal*. pp. 405–414. <https://doi.org/10.2134/agronj2006.0027>
- FAO, 2015. World fertilizer trends and outlook to 2018, Food and Agriculture Organization of United Nations.
- FAO, 2014. Building a common vision for sustainable food and agriculture. PRINCIPLES AND APPROACHES.
- Garnett, T., Appleby, M.C., Balmford, A., Bateman, I.J., Benton, T.G., Bloomer, P., Burlingame, B., Dawkins, M., Dolan, L., Fraser, D., Herrero, M., Hoffmann, I., Smith, P., Thornton, P.K., Toulmin, C., Vermeulen, S.J., Godfray, H.C.J., 2013. Sustainable Intensification in Agriculture: Premises and Policies. *Science* (80-.). 341, 33–34. <https://doi.org/10.1126/science.1234485>
- Gitelson, A.A., Viña, A., Ciganda, V., Rundquist, D.C., Arkebauer, T.J., 2005. Remote estimation of canopy chlorophyll content in crops. *Geophys. Res. Lett.* 32, 1–4. <https://doi.org/10.1029/2005GL022688>
- Goulding, K., Jarvis, S., Whitmore, A., 2008. Optimizing nutrient management for farm systems. *Philos. Trans. R. Soc. B Biol. Sci.* 363, 667–680. <https://doi.org/10.1098/rstb.2007.2177>
- Hatfield, J.L., Gitelson, A.A., Schepers, J.S., Walthall, C.L., 2008. Application of spectral remote sensing for agronomic decisions. *Agron. J.* <https://doi.org/10.2134/agronj2006.0370c>
- Holland, K.H., Schepers, J.S., 2010. Derivation of a variable rate nitrogen application model for in-season fertilization of corn. *Agron. J.* 102, 1415–1424.
- Justes, E., Jeuffroy, M., Mary, B., 1997. Wheat, Barley and Durum Wheat, in: Lemaire, G. (Ed.), *Diagnosis of the Nitrogen Status in Crops*. Springer-Verlag, Berlin, Heidelberg, pp. 73–91.
- Kemarian, A.R., Stöckle, C.O., Huggins, D.R., Viega, L., 2007. A simple method to estimate harvest index in grain crops. *F. Crop. Res.* 103, 208–216. <https://doi.org/10.1016/j.fcr.2007.06.007>
- Peralta, N.R., Costa, J.L., Balzarini, M., Castro Franco, M., Córdoba, M., Bullock, D., 2015. Delineation of management zones to improve nitrogen management of wheat. *Comput. Electron. Agric.* 110, 103–113. <https://doi.org/10.1016/j.compag.2014.10.017>
- Ritchie, J.T., Singh, U., Godwin, D.C., Bowen, W.T., 1998. Cereal growth, development and yield. *Underst. options Agric. Prod.* 79–98. https://doi.org/10.1007/978-94-017-3624-4_5
- Sadras, V.O., Connor, D.J., 1991. Physiological basis of the response of harvest index to the fraction of water transpired after anthesis: A simple model to estimate harvest index for determinate species. *F. Crop. Res.* 26, 227–239. [https://doi.org/10.1016/0378-4290\(91\)90001-C](https://doi.org/10.1016/0378-4290(91)90001-C)